IEEE Access
Multidisciplinary | Rapid Review | Open Access Journal

Received February 9, 2019, accepted February 22, 2019, date of publication February 28, 2019, date of current version March 20, 2019.

Digital Object Identifier 10.1109/ACCESS.2019.2902169

Orthogonal Projection With Optimized Reserved Subcarriers Mapping for Sidelobe Suppression in OFDM Systems

GUANGFA DAI[1,2], SHAOPING CHEN[2], (Member, IEEE), AND GAOFENG WANG[3], (Senior Member, IEEE)

[1]School of Electronic Information, Wuhan University, Wuhan 430074, China
[2]Hubei Key Laboratory of Intelligent Wireless Communications, South Central University for Nationalities, Wuhan 430074, China
[3]College of Electronics and Information, Hangzhou Dianzi University, Hangzhou 310000, China

Corresponding author: Shaoping Chen (spchen@scuec.edu.cn)

This work was supported in part by the National Natural Science Foundation of China under Grant 61571467, Grant 61801523, and Grant 61302117, and in part by the Fundamental Research Funds for the Central Universities under Grant SCUEC-CZY18045.

ABSTRACT As an efficient sidelobe suppression technique for orthogonal frequency-division multiplexing (OFDM) systems, the orthogonal projection is capable of achieving deep suppression while maintaining low complexity. However, the conventional orthogonal projection for sidelobe suppression (SSOP) with the uniform distribution of reserved subcarriers suffers from noise amplification in data recovery, resulting in a degradation of bit-error-rate (BER) performance. To tackle this problem, an improved SSOP with an optimized mapping of reserved subcarriers (SSOP-OM) is proposed in this paper. Additionally, a fast search algorithm is proposed to obtain this optimized distribution. By maximizing the signal-to-noise ratio (SNR) at the receiver, SSOP-OM can obtain more than 3-dB SNR gain for a 16-QAM-modulated OFDM system with 128 subcarriers and 6 of them reserved over conventional SSOP at the BER of 10^{-3}. In addition, the more reserved subcarriers or the more subcarriers are used in the OFDM, the higher the SNR gain can be achieved. The theoretical analysis and simulations are provided to validate the advantage of the proposed SSOP-OM over the conventional SSOP in terms of BER in both AWGN and multipath channels.

INDEX TERMS OFDM, sidelobe suppression with orthogonal projection (SSOP), noise amplification, optimized mapping of reserved subcarriers.

I. INTRODUCTION

Orthogonal frequency division multiplexing (OFDM) has been widely used in various broadband communications [1], [2] due to its high spectrum efficiency and low complexity equalization in multipath channels. However, due to its inherent nature of *sinc* waveform in spectrum, OFDM suffers from high sidelobe emissions, which will interfere with systems operating in adjacent bands if it is not properly suppressed. In non-contiguous OFDM (NC-OFDM) that is employed as a physical layer candidate of cognitive radio where the scattered spare spectrum of NC-OFDM based primary systems may be used by intelligent secondary systems, out-of-band (OOB) radiation needs to be suppressed in a depth of more than 60dB [3]. To this end, various techniques have been proposed, including windowing [4], active interference cancellation (AIC) [5], extended AIC (EAIC) [6] and spectrum coding [7]. Windowing is an efficient technique for the reduction of OOB radiation with a low complexity. However, it necessitates an insertion of additional guard intervals besides commonly used cyclic prefix (CP), which will result in a reduced spectrum efficiency. AIC [5] employs specifically designed cancellation signals loaded on the reserved orthogonal subcarriers, called cancellation subcarriers (CC), to cancel the sidelobes of data signals that are transmitted on the remaining subcarriers. AIC is very effective for sidelobe cancellation, but it also reduces spectrum efficiency due to the fact that a large number of CCs have to be reserved for a satisfactory performance of OOB suppression to be achieved. The available subcarriers left for data transmission are therefore reduced. To achieve a deeper notch of sidelobe suppression without use of more orthogonal CCs, an extended

The associate editor coordinating the review of this manuscript and approving it for publication was Daquan Feng.

AIC (EAIC) was proposed in [6] by employing more cancellation signals where some of them are loaded on the orthogonal subcarriers and others on the non-orthogonal one. EAIC achieves a significant gain, but the CC signals inserted on non-orthogonal subcarriers will introduce interference to subcarriers used for data transmission, resulting in a degradation of bit error performance. Besides, the high energy of cancellation signals used for OOB suppression reduces the power efficiency of OFDM systems, which is not desirable for system design. To achieve a deeper notch of sidelobe suppression while reducing the interference to data subcarriers at the same time, two improved AIC methods have been proposed in [8] and [9] via optimizing the CC locations and power allocation to cancellation signals. In addition, a technique that combines AIC (EAIC) with filtering processing was proposed in [10] to achieve better OOB suppression performance at a cost of high computational complexity. Ni *et al.* [11] used a joint optimization method to achieve both sidelobe cancellation and peak-to-average power ratio (PAPR) reduction.

In addition, a spectrum coding method was proposed in [7] to suppress OOB radiation in OFDM by employing specifically designed coding matrices. Later, many spectrum coding methods were put forward in [12]–[17] for a better performance at a cost of increased complexity or degraded bit error rate (BER) performance. Recently, some techniques, e.g., matrix decomposition [18], block reflector [19], matrix **WY** representation [20], and QR-decomposition [21] were employed to reduce the computational complexity of the orthogonal precoding [14], [15]. However, additional computational complexity is introduced under cognitive radio scenario [20]. In addition, a sidelobe suppression with orthogonal projection (SSOP) was proposed in [22] to allow a trade-off between the BER performance and computational complexity for zero padding OFDM (ZP-OFDM) system. SSOP has also been employed in a multi-band OFDM system [23].

However, SSOP suffers from the problem of noise amplification, which will degrade BER performance, because conventional SSOP employs uniform reserved subcarriers mapping that may introduce noise amplification at the data recovery. In this paper, SSOP with optimized mapping of reserved subcarriers (SSOP-OM) is proposed to maximize the SNR of the received signal, which will alleviate noise amplification and an obviously lower error rate can be achieved. In addition, a fast search algorithm is proposed to obtain the optimized distribution. The more reserved subcarriers (or more subcarriers in the OFDM) are used, the higher SNR gain can be achieved in SSOP-OM. It is noted that SSOP-OM achieves the same level of OOB suppression as conventional SSOP since both employ the same projection matrix and similar OOB processing techniques although they have different allocations of reserved subcarriers.

Notation: Lower-case bold face variables ($\mathbf{a}$, $\mathbf{b}$) indicates column vectors, and upper-case bold face variables ($\mathbf{A}$, $\mathbf{B}$) indicates matrices. $\mathbf{I}$ denotes the identity matrix, Tr means trace of matrix, $(\cdot)^T$, $(\cdot)^*$, $(\cdot)^{-1}$, $(\cdot)^\dagger$ denotes transposition, conjugate transposition, inverse and pseudo-inverse, respectively. $\mathbf{A}[S, :]$ and $\mathbf{A}[:, T]$ denote the sub-matrices of $\mathbf{A}$ with the rows specified with index set S, and the columns specified with index set T, respectively. $\mathbf{A}[S, T]$ denotes the sub-matrix of matrix $\mathbf{A}$ with the rows and columns specified with index set S and T, respectively.

II. SYSTEM MODEL AND SSOP ALGORITHM FOR OFDM

To facilitate the later development, we first review in brief the system model and SSOP algorithm for OFDM [22].

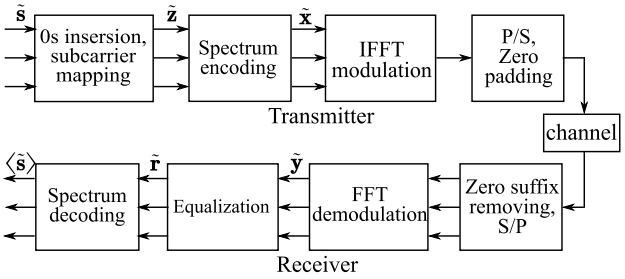

FIGURE 1. System diagram of ZP-OFDM system with SSOP.

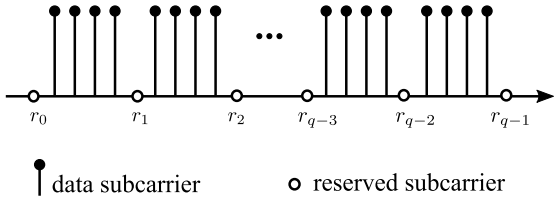

FIGURE 2. Distribution of data and reserved subcarriers in SSOP.

A. OFDM TRANSMITTER WITH CONVENTIONAL SSOP

An OFDM system with SSOP is considered, as shown in Fig. 1, where $M - q$ of the M subcarriers are used for transmitting data block $\tilde{\mathbf{s}} \in \mathbb{C}^{M-q}$, which are obtained from modulation mapping and serial-to-parallel (S/P) transformation, and q subcarriers are reserved for sidelobe suppression (transmitting 0). The reserved subcarriers are uniformly distributed among groups of data subcarriers, as shown in Fig. 2, such that the transmitted data can be recovered at the receiver with a low complexity SSOP decoder. Specifically, the subcarriers reserved are those with index set $S_r = \{r_0, r_1, r_2, \cdots, r_{q-1}\} = \{0, v, 2v, \cdots, M - v - 1, M - 1\}$, where $v = floor(\frac{M}{q-1})$ with $floor(a)$ denoting the greatest integer less than or equal to a. The symbol block $\tilde{\mathbf{z}}$ of length M after the insertion of 0s at reserved subcarriers is processed by SSOP precoding for sidelobe suppression before OFDM modulation at the transmitter. The result is

$$\tilde{\mathbf{x}} = \sqrt{\lambda}\mathbf{P}\tilde{\mathbf{z}}, \tag{1}$$

where $\mathbf{P} \in \mathbb{R}^{M\times M}$ is the precoding matrix and can be obtained [22] as $\mathbf{P} = \mathbf{I} - \mathbf{C}(\mathbf{C}^T\mathbf{C})^{-1}\mathbf{C}^T$ by solving the problem of forcing the out-band emission at frequencies f_k, $0 \le k \le p-1$, to be zero, where $\mathbf{C} \in \mathbb{R}^{M\times p}$ has elements $\mathbf{C}[m,k] = 1/|m - f_kT|$ for $m \ne f_kT$ and $\mathbf{C}[m,k] = 1$ for $m = f_kT$, where T is the length of OFDM signal before zero padding (ZP), the factor λ is introduced so that the

mean power of the transmitted data is normalized to 1 [22]. After IFFT modulation and ZP insertion, the obtained signal is transmitted through a channel. The larger p, the more frequencies at which the spectrum is suppressed to zero, and a deeper notch of the out-of-band suppression is achieved. To enable the data recovery at the receiver, $\mathbf{C}_r$ should have a full column rank and $p = q$ holds [22]. There exists a trade-off between the sidelobe suppression performance and the subcarriers available for data transmission (spectrum usage). In practice, $p = q \ll M$, meaning that cost of spectrum efficiency is small for a satisfied suppression performance to be achieved.

B. DATA RECOVERY AT THE RECEIVER

At the receiver, the received signal after ZP-OFDM demodulation [22] can be expressed as

$$\tilde{\mathbf{y}} = \mathbf{D}\tilde{\mathbf{x}} + \tilde{\mathbf{n}} = \sqrt{\lambda}\mathbf{D}\mathbf{P}\tilde{\mathbf{z}} + \tilde{\mathbf{n}}, \tag{2}$$

where $\mathbf{D}$ is a diagonal matrix with diagonal elements, $H = \{H_0, H_1, \cdots, H_{M-1}\}$, being the frequency-domain responses of the multipath channel [24], $\tilde{\mathbf{n}}$ is AWGN noise with zero mean and variance σ_n^2. When a zero forcing (ZF) equalizer is applied, we obtain

$$\tilde{\mathbf{r}} = \frac{1}{\sqrt{\lambda}}\mathbf{D}^{-1}\tilde{\mathbf{y}} = \mathbf{P}\tilde{\mathbf{z}} + \frac{1}{\sqrt{\lambda}}\mathbf{D}^{-1}\tilde{\mathbf{n}}. \tag{3}$$

Equation (3) can be split into two equations as [22]

$$\tilde{\mathbf{r}}_d = \tilde{\mathbf{s}} - \mathbf{C}_d(\mathbf{C}^T\mathbf{C})^{-1}\mathbf{C}_d^T\tilde{\mathbf{s}} + \mathbf{D}_d^{-1}\tilde{\mathbf{n}}_d/\sqrt{\lambda}, \tag{4}$$

$$\tilde{\mathbf{r}}_r = -\mathbf{C}_r(\mathbf{C}^T\mathbf{C})^{-1}\mathbf{C}_d^T\tilde{\mathbf{s}} + \mathbf{D}_r^{-1}\tilde{\mathbf{n}}_r/\sqrt{\lambda}, \tag{5}$$

where $\tilde{\mathbf{r}}_r \in \mathbb{C}^q$ and $\tilde{\mathbf{r}}_d \in \mathbb{C}^{M-q}$ denote the sub-vectors constructed from the elements of corresponding to the reserved subcarriers and data subcarriers, respectively; $\mathbf{C}_r \in \mathbb{R}^{q\times p}$ and $\mathbf{C}_d \in \mathbb{R}^{(M-q)\times p}$, $\mathbf{D}_r \in \mathbb{C}^{q\times q}$ and $\mathbf{D}_d \in \mathbb{C}^{(M-q)\times(M-q)}$, $\tilde{\mathbf{n}}_r \in \mathbb{C}^q$ and $\tilde{\mathbf{n}}_d \in \mathbb{C}^{M-q}$ are the sub-matrices or sub-vectors obtained from the partitioning of the corresponding $\mathbf{C}$, $\mathbf{D}$ and $\tilde{\mathbf{n}}$, respectively, in the same manner. From equations (4) and (5), we obtain the estimated data as [22]

$$\begin{aligned}\langle\tilde{\mathbf{s}}\rangle &= \tilde{\mathbf{r}}_d - \mathbf{C}_d(\mathbf{C}_r)^\dagger\tilde{\mathbf{r}}_r \\ &= \tilde{\mathbf{s}} + \mathbf{D}_d^{-1}\tilde{\mathbf{n}}_d/\sqrt{\lambda} - \mathbf{C}_d(\mathbf{C}_r)^\dagger\mathbf{D}_r^{-1}\tilde{\mathbf{n}}_r/\sqrt{\lambda}\end{aligned} \tag{6}$$

where ${\mathbf{C}_r}^\dagger = (\mathbf{C}_r^T\mathbf{C}_r)^{-1}\mathbf{C}_r^T$ is a pseudo-inverse of $\mathbf{C}_r$.

C. NOISE AMPLIFICATION ASSOCIATED WITH DATA RECOVERY

In the right-hand side of (6), the first term is the desired signal, the second is effect of noise on the data subcarrier, and the third is the effect of noise on the reserved subcarriers. The third term may introduce noise amplification, which will degrade the error rate performance of OFDM system, and is therefore the focus of our analysis. From (6), we obtain the signal to noise ratio (SNR) as

$$SNR = \frac{\lambda\sigma_s^2(M-q)}{\sigma_n^2\left(\mathrm{Tr}((\mathbf{D}_d\mathbf{D}_d^*)^{-1}) + \mathrm{Tr}((\mathbf{D}_r^*\mathbf{D}_r)^{-1}(\mathbf{C}_d(\mathbf{C}_r)^\dagger)^T\mathbf{C}_d(\mathbf{C}_r)^\dagger)\right)} \tag{7}$$

where σ_s is variance of transmitted data. In the OFDM without SSOP, the term $\mathrm{Tr}\left((\mathbf{D}_r^*\mathbf{D}_r)^{-1}(\mathbf{C}_d(\mathbf{C}_r)^\dagger)^T\mathbf{C}_d(\mathbf{C}_r)^\dagger\right)$ introduced by SSOP precoding does not exist. For $\mathrm{Tr}\left((\mathbf{D}_r^*\mathbf{D}_r)^{-1}(\mathbf{C}_d(\mathbf{C}_r)^\dagger)^T\mathbf{C}_d(\mathbf{C}_r)^\dagger\right) > 0$, SSOP precoding will degrade the received SNR, resulting in the BER performance degradation. It was shown in [22] that conventional SSOP precoding will introduce about 3dB SNR degradation for $q = 4$ and $M = 64$ in AWGN channels. To alleviate this problem, Zhang *et al.* [22] proposed a nulling method, where the signals in (6) are first transformed to time domain using an IDFT and the samples in the IDFT output subject to larger noise power are then nulled out (set to zeros) and the results are finally transformed back to frequency domain using a DFT for data recovery. The transformation between time- and frequency-domain will introduce additional computational burden. Meanwhile, the nulling processing in [22] suffers from a SNR threshold problem due to the loss of data energy that is leaked to the reserved subcarriers. Specifically, under the low SNR condition, the noise power is larger than the signal power on the reserved subcarriers, the nulling method in [22] can therefore obtain an obvious BER gain. In a high SNR, however, nulling operation will significantly degrade BER performance since signal energy leaked to the reserved subcarriers is larger than that of noise. The BER simulation results in [22, Fig. 8] agree with our analysis. Moreover, the noise amplification will become more serious when M and q are large for a higher transmission rate and a better spectral sidelobe suppression to be achieved.

In the following, we will present an optimized reserved subcarriers mapping for SSOP based on SNR maximization, which is capable of significantly alleviating the problem of noise amplification by exploiting the characteristics of the auxiliary signal.

III. OPTIMIZED SSOP WITH MAXIMIZED SNR

The key to tackle the problem of noise amplification is to significantly boost the SNR of the estimated signal $\langle\tilde{\mathbf{s}}\rangle$ in (6). To this end, we propose an improved SSOP with optimized reserved subcarriers distribution based on SNR maximization while maintaining the same performance of sidelobe suppression. It is noted from (1) that the notches of sidelobe suppression is determined by the precoding matrix $\mathbf{P} = \mathbf{I} - \mathbf{C}(\mathbf{C}^T\mathbf{C})^{-1}\mathbf{C}^T$ or by matrix $\mathbf{C} \in \mathbb{R}^{M\times p}$. The larger the p is, the more frequencies at which the spectrum are suppressed to zero, and the deeper notch of OOB suppression is achieved. It implies that it is the number, p, and positions of frequencies at which the spectrum is forced to zero that will determine the performance of sidelobe suppression performance no matter how the reserved subcarriers are distributed. In fact, the pattern of reserved subcarriers distribution will determine the power of the introduced noise on the reserved subcarriers in (6), SNR of estimated signal defined by (7) and the BER performance of data recovery. The focus of our design is to search for the optimized distribution of reserved subcarriers, $\hat{S}_r$, that maximizes the SNR of estimated signal

for a fixed M and q (number of reserved subcarriers). For $q \ll M$, $\lambda = 1/\left(\sigma_s^2\left(M - q - \mathrm{Tr}\left(\mathbf{C}_d\left(\mathbf{C}^T\mathbf{C}\right)^{-1}\mathbf{C}_d^T\right)\right)\right) \cong 1/\left(\sigma_s^2(M-q)\right)$ holds [22], meaning λ to be a constant for fixed M and q regardless of the distribution of reserved subcarriers $S_r = \{r_0, r_1, r_2, \cdots, r_{q-1}\}$. The optimization problem can be formulated as

$$\begin{aligned}
&\min_{S_r} \alpha = f(S_r)\\
&\text{s.t. } S_r = \{r_0, r_1, \cdots, r_{q-1}\} \subset \{1, 2, \cdots, M-1\},\\
&\quad S_d = \{d_0, d_1, \cdots, d_{M-q-1}\} \subset \{1, 2, \cdots, M-1\},\\
&\quad S_r \cup S_d = \{0, 1, 2, \cdots, M-1\},\\
&\quad S_r \cap S_d = \emptyset. \qquad (8)
\end{aligned}$$

where

$$\begin{aligned}
f(S_r) &= \mathrm{Tr}\left((\mathbf{D}_d\mathbf{D}_d^*)^{-1}\right)\\
&\quad + \mathrm{Tr}\left((\mathbf{D}_r^*\mathbf{D}_r)^{-1}(\mathbf{C}_d(\mathbf{C}_r)^\dagger)^T\mathbf{C}_d(\mathbf{C}_r)^\dagger\right) \qquad (9)\\
\mathbf{C}_r &= \mathbf{C}[S_r, :] \qquad (10)\\
\mathbf{C}_d &= \mathbf{C}[S_d, :] \qquad (11)\\
\mathbf{D}_r &= \mathbf{D}[S_r, S_r] \qquad (12)\\
\mathbf{D}_d &= \mathbf{D}[S_d, S_d] \qquad (13)
\end{aligned}$$

$\mathbf{C}_r$ is a $q \times p$ sub-matrix of $\mathbf{C}$ with its rows collected from the rows of $\mathbf{C}$ which are specified with index set S_r; $\mathbf{C}_d$ is an $(M-q)\times p$ sub-matrix of $\mathbf{C}$ obtained by removing $\mathbf{C}_r$ from $\mathbf{C}$; $\mathbf{D}_r$ and $\mathbf{D}_d$ are similarly defined. This is a combinatorial (or discrete) optimization problem, where $\alpha = f(S_r)$ is a quadratic function of discrete parameter S_r, the index set of the reserved subcarriers. Although it is easy to obtain a closed form solution for continuous parameters, it is difficult to find one for such a combinatorial optimization problem with discrete parameters. The widely used method to solve this problem is the exhaustive search [25], where all possible combinations are examined to find the discrete S_r such that the smallest α is achieved. Exhaustive search may be acceptable when both M and q are small, but it will become intolerable for large M and q due to the explosive increase of complexity. To reduce the search complexity, we design a fast search algorithm by making use of the symmetry of $\mathbf{C}$ and by transforming a complex multivariate optimization problem into a series of low complexity ones. Similar problems have been investigated in [8] and [9]. Note that we have not taken into account the pilot subcarriers in our design as those in [18]–[20] and [22] for the sake of simplicity and for the convenience of comparison, but it is straight forward to extend our design to the OFDM with pilot subcarriers.

We observe that the matrix $\mathbf{C}$ has a symmetry feature, i.e., $\mathbf{C}_{k,j} = \mathbf{C}_{M-k,q-j}$. Since the optimal $\mathbf{C}_r$ also has this symmetry characteristics, we conclude that $r_k + r_{M-k} = M - 1$ will facilitate the search for optimized distribution. Meanwhile, the values of elements in each column of $\mathbf{C}$ vary monotonically from the top to the bottom. Thus, a local optimum can be easily reached within a few steps of search in each single variable optimization problem. Although the optimal distribution is not uniform due to the quadratic optimization function, we may begin our search from the uniform distribution and towards the direction of decreasing α.

A. AWGN CHANNEL

In the AWGN channel, both $\mathbf{D}_d$ and $\mathbf{D}_r$ are identity matrix, (9) is simplified into

$$f(S_r) = \mathrm{Tr}\left((\mathbf{C}_d(\mathbf{C}_r)^\dagger)^T\mathbf{C}_d(\mathbf{C}_r)^\dagger\right). \qquad (14)$$

Since $q \ll M$, it is possible to obtain the optimal solution, $\hat{S}_r$, through an offline exhaustive search. Once we have the solution, we can store it for precoder design. Thus, the proposed scheme will have the same online computational complexity as the conventional SSOP.

B. MULTIPATH CHANNEL

For time-varying multipath channels where channel state varies from OFDM block to block but is assumed to remain unchanged during an OFDM interval, the optimal reserved subcarrier distribution varies accordingly and needs to be updated repeatedly. If the exhaustive search is employed, α will need to be calculated $\binom{M}{q} = \frac{M!}{q!(M-q)!}$ times for each channel state. The computation complexity will become unacceptable for large M and q. To alleviate this problem, we propose a fast search algorithm employing an iterative strategy that will reduce the computational complexity exponentially. The algorithm is described in algorithm 1.

The key of fast search is to convert the combinatorial optimization problem into a series of simple optimization ones that can be easily solved by iterative processing. Specifically, at the beginning of the iteration, the optimized reserved subcarrier distribution for the i-th OFDM symbol, $S_r^{(i)}$, is initialized with a given distribution, $S_{\mathrm{ini}}^{(i)}$, which is either a uniform distribution, S_u, or the optimized distribution obtained for the previous OFDM symbol, $S_r^{(i-1)}$, if it is available. In each cycle of iteration, two steps are employed to find a more converged result and then the optimized one is achieved after several iterations. In step one, a variable, r_k, is chosen from S_r that will lead to the greatest change to $\alpha^{(i)}$ within one step. In step two, the value of r_k is updated by keeping r_k moving in the direction that the value of $\alpha^{(i)}$ will be decreased. After no more than p cycles of iterations, the optimized $S_r^{(i)}$ will be obtained.

It is noted that our scheme still has a low complexity despite of the iterative search for the solution. This can be explained as follows. First, the computation complexity of the algorithm 1 is not so high. Generally, this algorithm can find the optimal $S_r^{(i)}$ within less than p iterations and a few calculations of α are needed in each iteration. Second, we may further reduce the computational complexity by making use of the results obtained in the previous OFDM symbols, $S_r^{(i-1)}$, as depicted in Fig. 3. Specifically, for case 1, for the first OFDM symbol, the $S_r^{(i)}$ is initialized with the uniform distribution S_u. For case 2, where the channel varies slowly in two consecutive OFDM symbols such that the correlation

Algorithm 1 Fast Search Algorithm for Optimized Reserved Subcarriers Distribution of the i-th OFDM Symbol

Input: frequency domain channel response for the i-th OFDM symbol $H^{(i)}$,
Initial value of the reserved subcarrier distribution $S_{\text{ini}}^{(i)}$
Output: Optimized reserved subcarrier distribution $S_r^{(i)}$

Initialization: $S_r^{(i)} \leftarrow S_{\text{ini}}^{(i)}$
for $ite = 1$ **to** p **do**
  Compute $\alpha_0 = f(S_r^{(i)})$ using (9)
  for $m = 1$ **to** $p//2 - 1$ **do**
    $S_r^m \leftarrow S_r^{(i)}$
    Update S_r^m with $r_m \leftarrow r_m + 1$ and $r_{M-m-1} \leftarrow r_{M-m-1} + 1$
    Compute $\alpha_m = f(S_r^m)$
    $\Delta\alpha_m = \alpha_m - \alpha_0$
  end for
  $k \leftarrow \underset{m\in\{1,\cdots,p//2-1\}}{\arg\max} |\Delta\alpha_m|$
  $direction = \text{sign}(\Delta\alpha_k)$
  $\alpha_{old} \leftarrow \alpha_0$
  repeat
    Update $S_r^{(i)}$ with $r_k \leftarrow r_k - direction \cdot \gamma$ and $r_{M-k-1} \leftarrow r_{M-k-1} - direction \cdot \gamma$
    Compute $\alpha_{new} = f(S_r^{(i)})$
    $\Delta\alpha = \alpha_{new} - \alpha_{old}$
    $\alpha_{old} \leftarrow \alpha_{new}$
  until $\Delta\alpha > 0$
  if $|\alpha_0 - \alpha_{new}| < \epsilon$ **then**
    break
  end if
end for

coefficient between the channel response of the current OFDM symbol $H^{(i)}$ and that of the previous OFDM symbol $H^{(i-1)}$ is larger than a predefined threshold, δ, (Actually, this condition is satisfied most cases and δ can be determined by simulations), the $S_r^{(i-1)}$ obtained for the former OFDM symbol can be directly used for the current OFDM symbol and no search is needed. Otherwise, the optimized distribution $S_r^{(i-1)}$ for the previous OFDM symbol may be used as initialization value to search for the optimized $S_r^{(i)}$ for the current OFDM symbol. In this way, convergence rate of algorithm 1 can be greatly sped up.

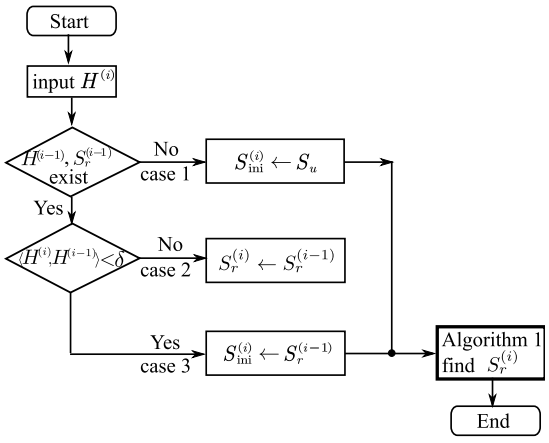

FIGURE 3. Flowchart of the search and updating optimized reserved subcarrier distribution.

TABLE 1. Computational complexity for calculating α in multipath channels.

Step	Number of real multiplications
$(\mathbf{C}_r)^\dagger = (\mathbf{C}_r^T\mathbf{C}_r)^{-1}\mathbf{C}_r^T$	$3q^3$
$(\mathbf{C}_r)^\dagger\mathbf{D}_r^{-1}$	q^2+q
$\mathbf{B} = \mathbf{C}_d(\mathbf{C}_r)^\dagger\mathbf{D}_r^{-1}$	$(M-q)\,q^2$
$\text{Tr}\left(\mathbf{B}^T\mathbf{B}\right)$	$(M-q)\,q$
$\text{Tr}\left((\mathbf{D}_d\mathbf{D}_d^*)^{-1}\right)$	$2\,(M-q)$
Total	$(M-q)\,(q^2+q+2)+3q^3+q^2+q$

IV. COMPLEXITY ANALYSIS

The proposed SSOP-OM has the same encoding matrix and the same decoding processing as the conventional SSOP spectrum encoder. The main difference is the distribution of their reserved subcarriers, i.e., the conventional SSOP employs uniformly distributed reserved subcarriers and no search is needed for uniform distribution while the proposed SSOP-OM employs the optimized distribution of reserved subcarriers and a search is required to find this optimized distribution. In this section, we will first calculate the extra computational complexity needed in SSOP-OM to find the optimized distribution of reserved subcarriers, and then analyze the total computational complexity.

For AWGN channel, optimized distribution of reserved subcarriers can be obtained offline by exhaustive search or fast search in advance and remains the same for all OFDM symbols. The on-line computational complexity for encoding and decoding are about $2(2M-q)q$ and $(2M-q)q$ times of real multiplications, respectively, which are the same as the conventional SSOP [22].

For time-varying multipath channels, it is necessary to search for the optimized distributions repeatedly according to channel condition using search algorithm 1. The computational burden of algorithm 1 is mainly caused by the repeated calculations of the objective function $\alpha = f(S_r)$, defined by (9), according to the candidate distributions of reserved subcarriers, S_r, where $(M-q)(q^2+q+2)+3q^3+q^2+q$ multiplications are required for calculation of each α, as shown in Table 1, which is approximately Mq^2, for $q \ll M$. However, the times of computing α may be different to achieve the optimal distribution for different channel states according to Fig. 3. We evaluate the average times of calculating α for each OFDM symbol, denoted by ρ, via simulations. In section V-B, we find that, under the time-varying channel with the Doppler frequency shift 100Hz, ρ is no more than 0.041. Considering that $\rho \ll 1$ and $q \ll M$, the extra computations required for SSOM-OP, ρMq^2, is trivial compared with the computation burden for the conventional SSOP, $2(2M-q)q$. The complexity comparison

TABLE 2. Complexity comparison among spectrum precodings.

	Real multiplications for encoding	Real multiplications for decoding
[14], [15]	$4M\,(M-q)$	$4M\,(M-q)$
[18]	$8\,(2M-q)\,q$	$8\,(2M-q)\,q$
[19]–[21]	$4\,(2M-q)\,q$	$4\,(2M-q)\,q$
SSOP [22]	$2(2M-q)q$	$(2M-q)q$
SSOP-OM	$2(2M-q)q+\rho^a Mq^2$	$(2M-q)q$

[a] $\rho \leq 0.041$ according to Table 4, section V-B.

among SSOP, SSOP-OM, and other spectral encoders are listed in Table 2. It shows that the online real multiplications required for SSOP-OM, $2(2M-q)q+\rho Mq^2$, is very close to that for the conventional SSOP [22] and much less than those for other spectrum encoders [15], [18]–[21]. Furthermore, the SSOP-OM can avoid the additional computational complexity for matrix decomposition needed in these spectrum encoders [18]–[21] under cognitive radio scenario.

It should be noted that the transmitter does not have to send the optimal S_r to the receiver. The reason is that the positions of reserved subcarriers used at the transmitter can be easily estimated by checking the power distribution at the receiver due to the fact that the power on reserved subcarrier is much lower than that on the data subcarriers in an OFDM system with SSOP-OM.

V. SIMULATIONS

In this section, simulations are provided to validate the effectiveness of the proposed SSOP-OM, including the optimized distribution of the reserved subcarriers and enhanced BER performance achieved by the proposed scheme. In the experiments, all the simulations were performed with the MATLAB software and its default double-precision float-point calculation. Monte Carlo simulations are used for the BER evaluation and the BER is estimated with the 10^8 transmitted OFDM symbols for each channel condition.

A. OPTIMIZED DISTRIBUTION OF THE RESERVED SUBCARRIERS IN AWGN CHANNEL

The optimized distribution of the reserved subcarriers of SSOP remains unchanged in AWGN channel. It can be obtained offline with exhaustive search or with the fast search algorithm. Both methods are provided for comparison in the simulations under AWGN channel. In algorithm 1, the search step length γ is set to 1, and the search termination parameter ϵ is set to 0.5. We consider two cases where the number of subcarriers M of the OFDM system is set to 64 and 128, respectively, and for each case, the number of reserved subcarriers q is set to 2, 4, 6, respectively. For $p = q = 2$, the two normalized frequencies at which the OOB emission is forced to be zero are $f_n = [-32, 95]$, where $f_n = fT$ is the frequency normalized to the length of OFDM symbol without ZP insertion. For $p = q = 4$ and $p = q = 6$, the normalized frequencies at which the OOB emission is forced to be zero are $f_n = [-64, -32, 95, 127]$ and $f_n = [-64, -32, -16, 87, 95, 127]$, respectively.

For $p = q = 2$, the reserved subcarriers are located at the edges: subcarrier 0 and subcarrier 63 for $M = 64$, or subcarrier 0 and 127 for $M = 128$, which are the same as the conventional SSOP. For $p = q = 4$ and $p = q = 6$, the distributions of the reserved subcarriers, S_r, the corresponding α, the online and offline multiplications required to search for S_r in different schemes are listed in Table 3.

It is observed from Table 3 that for AWGN channel, the distribution of reserved subcarriers obtained by exhaustive search (denoted as SSOP-OME) are not uniform and are located closer to edge subcarriers, which are different from the conventional SSOP. Meanwhile, although the α's obtained with fast search algorithm (denoted as SSOP-OM) are a bit larger than those obtained with the exhaustive search, they are much less than those with the uniform distribution. This implies that a significant higher SNR and therefore a better BER performance can be achieved with optimized distribution of reserved subcarriers in our proposed scheme. It is also observed that for a larger q (more reserved subcarriers are used) or for a larger number of subcarriers of OFDM, a higher SNR gain can be achieved with optimized distribution. Moreover, three schemes have the same online multiplication computations since they share the same spectrum encoding structure. In addition, a fast search algorithm can significantly reduce offline computations in SSOP-OM compared with the exhaustive search.

TABLE 3. Distributions of reserved subcarriers, the corresponding α and computations for AWGN channel.

		$q=4$				$q=6$			
		S_r	α	Online multiplications	Offline multiplications	S_r	α	Online multiplications	Offline multiplications
$M=64$	SSOP [22]	{0, 21, 42, 63}	119.7	992	0	{0, 13, 25, 38, 50, 63}	193.0	1464	0
	SSOP-OME	{0, 16, 47, 63}	110.6	992	6.51×10^8	{0, 6, 21, 42, 57, 63}	109.9	1464	1.73×10^{11}
	SSOP-OM	{0, 16, 47, 63}	110.6	992	8192	{ 0, 7, 25, 38, 56, 63}	120.3	1464	16128
$M=128$	SSOP [22]	{0, 42, 85, 127}	261.4	2016	0	{0, 25, 51, 76, 102, 127}	585.9	3000	0
	SSOP-OME	{0, 28, 99, 127}	226.8	2016	2.19×10^{10}	{0, 9, 39, 88, 118, 127}	230.4	3000	2.50×10^{13}
	SSOP-OM	{0, 28, 99, 127}	226.8	2016	34816	{ 0, 12, 51, 76, 115, 127}	278.6	3000	73728

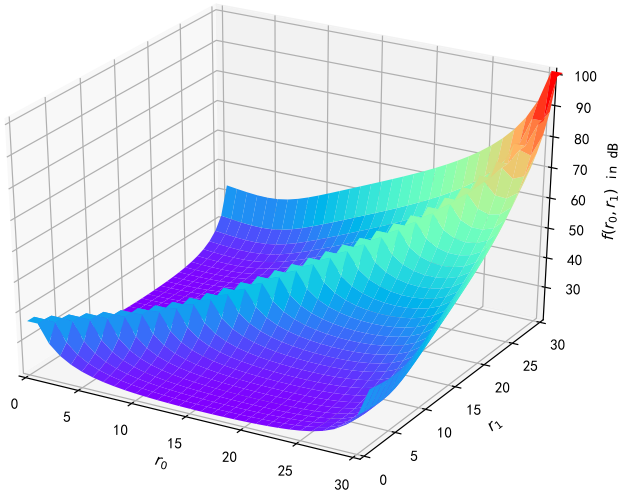

FIGURE 4. Function $f(r_1, r_2)$ plot in AWGN channel when $M = 64$, $q = 4$.

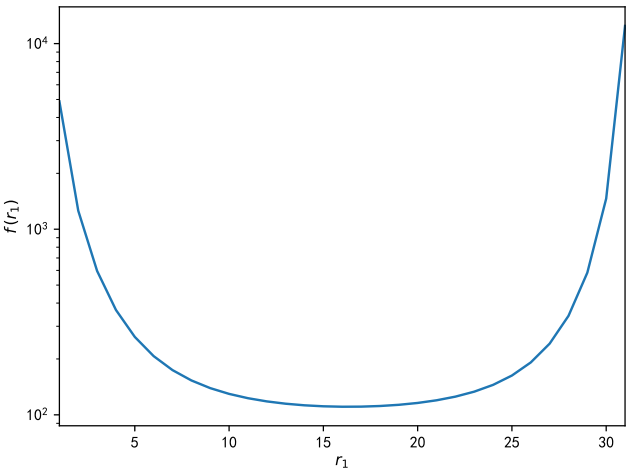

FIGURE 5. Function $f(r_1)$ plot in AWGN channel when $M = 64$, $q = 4$.

To more clearly illustrate the effect of reserved subcarriers distribution on the objective function $\alpha = f(S_r)$, we plot the surface of α, as an example, where $M = 64$, $q = 4$, in Fig. 4. The set of the locations of the 4 reserved subcarriers is denoted as $S_r = \{r_0, r_1, r_2, r_3\}$. Among the four parameters r_0, r_1, r_2, r_3, only two of them, such as r_0 and r_1, are independent due to the symmetry of S_r. So $f(S_r)$ can be reduced to a 3-dimensional surface $f(r_0, r_1)$ as shown in Fig. 4 for $0 \le r_0, r_1 \le M/2 - 1$. It can be seen that the surface is symmetrical with respect to the line $r_1 = r_0$. That is to say the α remains the same when r_0 and r_1 are interchanged. It also can be seen that the bottom of the surface is in the line of $r_0 = 0$ or $r_1 = 0$. It implies that the best reserved subcarrier distribution exists at two edge positions ($r_0 = 0$, $r_3 = M - 1$). In addition, it can be seen that α becomes very large near $r_0 = r_1$. This is due to the fact that the rows of $\mathbf{C}_r$ are more correlated when they are more closely spaced as expected. The result explains why the reserved subcarriers should be separated as far as possible in order to minimize the noise amplification at the receiver. Meanwhile, the bottom of the surface is closer to point (0,0) than to point (31, 31). This means that some reserved subcarriers should be positioned closer to the edge subcarriers.

Since two edge subcarriers are always chosen for reserved position, $f(S_r)$ is further simplified to function $f(r_1)$ in the case of $q = 4$, as shown in Fig. 5. We observe that for AWGN channels, the curve has an U shape with a bottom at $r_1 = 16$, which is different from the uniform distribution a bottom at $r_1 = 21$.

B. FAST SEARCH ALGORITHM UNDER MULTI-PATH CHANNEL

Different from AWGN channel, the optimized distribution of the reserved subcarriers is changing in time-varying multi-path channel. So, it is obtained in real time using fast search algorithm. In the simulations, we use a symbol spaced, delay line Jakes' model channel of 4 paths with an exponential delay power spectrum [26] and Doppler frequency shift $f_d = 100$Hz. The duration of the data part in OFDM symbol is 3.2us [1], and δ is set to 0.99 in algorithm 1. The other parameters remain the same as section V-A. Then α is averaged over 10^8 OFDM symbols (denoted by $\bar{\alpha}$). We estimate the average times of α calculation for each OFDM symbol, denoted by ρ, and the average online multiplications accordingly. The results are listed in Table 4.

It can be seen from Table 4 that, the optimized distribution using the fast search algorithm provides an obviously lower average $\bar{\alpha}$ than the uniform distribution. This implies that a higher SNR can be achieved with optimized distribution S_r, leading to a better BER performance for our proposed scheme. It also can be seen that for a larger q (more reserved subcarriers are used) or for a larger number of subcarriers of OFDM, a higher SNR gain can be achieved with optimized distribution. Meanwhile, the average times of α calculation for each OFDM symbol in SSOP-OM, denoted by ρ, are all no more than 0.041 and the average online computations for SSOP-OM are very close to those for the conventional SSOP. Therefore, the SSOP-OM has an obviously better SNR

TABLE 4. Average $\bar{\alpha}$, average times, ρ, of α calculation, and average real multiplications per OFDM symbol for different SSOP methods under time-varying channel with 100Hz Doppler frequency shift.

		$q = 4$			$q = 6$		
		$\bar{\alpha}$	ρ	Multiplications	$\bar{\alpha}$	ρ	Multiplications
$M = 64$	SSOP [22]	74.18	0	992	113.72	0	1464
	SSOP-OM	62.23	0.019	1012	62.55	0.041	1558
$M = 128$	SSOP [22]	113.72	0	2016	343.62	0	3000
	SSOP-OM	62.55	0.012	2041	129.2	0.022	3101

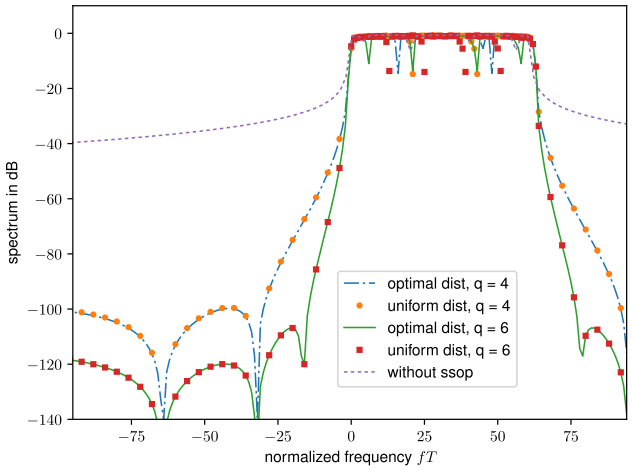

FIGURE 6. PSD for ZP-OFDM signals with different SSOP schemes, $M = 64$.

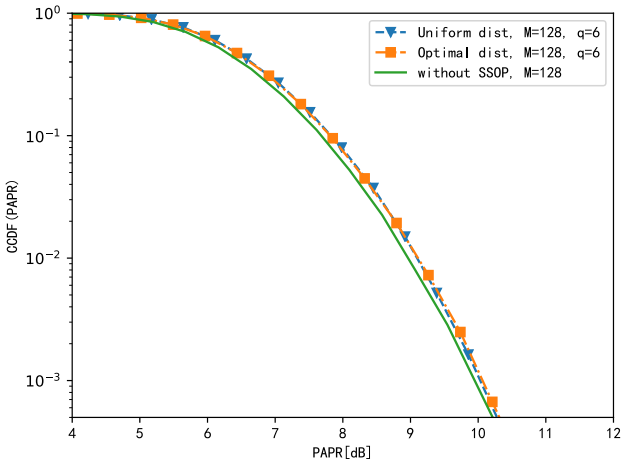

FIGURE 7. CCDF of PAPR for OFDM signals with different SSOP schemes.

performance at a cost of very low computation complexity in multi-path channel.

In addition, it can be seen that under the same value of q, the average times of α calculation for $M = 128$ are even less than those for $M = 64$. The reason is that the termination condition can be more easily met for a larger M or a larger q. Meanwhile, α decreases quickly at first and then slowly in the search, thus this termination parameter, ϵ, has limited impact on the α. If we use a smaller termination parameter ϵ and allow the algorithm to have more times of search when M and q are larger, then α will be further reduced and the search time will increase accordingly. This is a trade-off problem, and we will consider it in our future work.

C. SPECTRUM AND SIDELOBE SUPPRESSION PERFORMANCE

To illustrate the effectiveness of the proposed scheme, the power spectrum density (PSD) is calculated and plotted for comparison in Fig. 6, where $M = 64$. It is observed that for the same q (the number of reserved subcarriers), the same sidelobe suppression performance can be achieved for both uniform and optimized distribution of the reserved subcarriers. It can be explained by the fact that the sidelobe suppression depth depends upon the matrix $\mathbf{P}$ used in (1), which remains the same no matter how reserved subcarriers are distributed. For a larger q, a deeper notch of sidelobe suppression is achieved as expected.

Since SSOP spectrum coding introduces some correlation to the transmitted signal, it may slightly deteriorate the peak-to-average power ratio (PAPR) of the signal. In Fig. 7, the PAPR distributions of ZP-OFDM time-domain signals with two different reserved subcarrier distributions are presented, where $M = 128$, $q = 6$ and the oversampling factor is set to 4 in the computation of PAPR. It can be seen that the PAPR distributions for the two reserved subcarrier distributions are basically the same. The reason is that the PAPR's of time domain OFDM signal with SSOP are main determined by M and q regardless of the locations of the reserved subcarriers. Especially, when $q \ll M$, the PAPR distributions of the OFDM signal with SSOP are very close to that of conventional OFDM without spectrum coding. It is observed from Fig. 7 that the PAPR of OFDM in conventional SSOP and the proposed SSOP are slightly larger than that of the OFDM without SSOP. Obviously, this gap is almost negligible in practice.

D. BER PERFORMANCE

To illustrate the effectiveness of the proposed scheme in mitigating the effect of noise amplification, BER is simulated and plotted for comparison in this subsection.

1) AWGN CHANNEL

In the simulations, AWGN channels are assumed, 16QAM mapping is used, the number of OFDM subcarriers is $M = 64, 128$, and number of reserved subcarriers is $q = 2, 4, 6$. The results are shown as Fig. 8 and Fig. 9 and it is observed

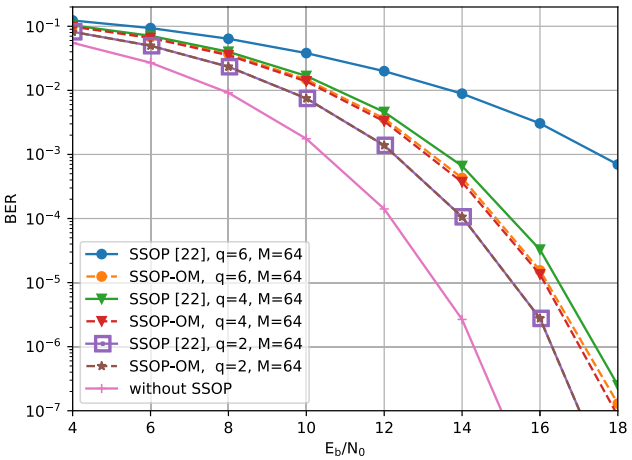

FIGURE 8. BER comparison in AWGN channel for 16-QAM, $M = 64$.

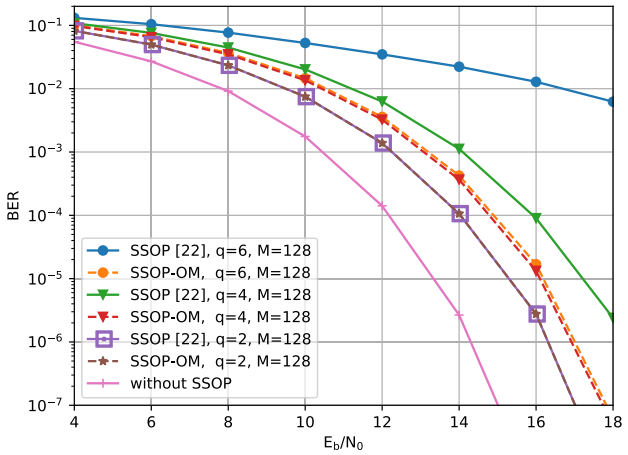

FIGURE 9. BER comparison in AWGN channel for 16-QAM, $M = 128$.

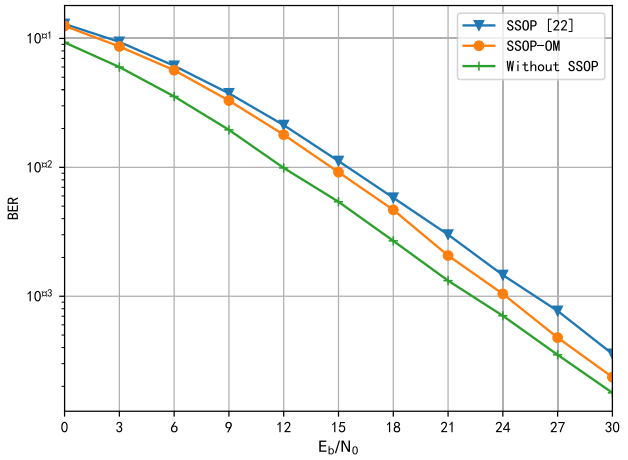

FIGURE 10. BER comparison in multipath channel for 16-QAM, $M = 64$, $q = 4$.

that the proposed SSOP-OM scheme obviously outperforms conventional SSOP in terms of BER. For a larger q or a larger M, more SNR gain is achieved and a more significant BER reduction is observed. For example, a SNR gain of more than 3dB is obtained under $q = 6$ at the BER of 10^{-3} regardless the value of M. It is noted that for $q = 2$, the same BER performance is observed since the proposed scheme has the same distribution as the conventional SSOP in this case.

2) MULTIPATH CHANNELS

Similar simulations and BER comparison are provided for the time-varying multipath channel in Fig. 10, where $M = 64$, $q = 4$ and in Fig. 11, where $M = 128$, $q = 6$. The parameters of the channel and OFDM system are the same as section V-B. For SSOP-OM scheme, the fast search algorithm is employed to search for the optimized reserved subcarrier distribution. Similar results are observed and the proposed SSOP-OM outperforms the conventional SSOP in terms of BER performance. For example, more than 3dB SNR gain is obtained with the optimized distribution of the reserved subcarriers when $M = 128$ and $q = 6$ over conventional one at various BER's.

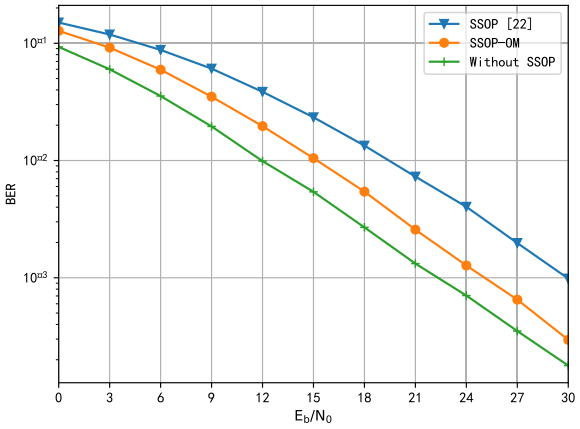

FIGURE 11. BER comparison in multipath channel for 16-QAM, $M = 128$, $q = 6$.

VI. CONCLUSION

A SSOP with optimized mapping of reserved subcarriers (SSOP-OM) and its fast search algorithm are proposed in this paper. Compared to the conventional SSOP with the uniform distribution of reserved subcarriers, SSOP-OM achieves a significant SNR gain and lower BER performance in both AWGN and multipath channels while maintaining the same sidelobe suppression performance. Moreover, the more reserved subcarriers, or the more subcarriers for OFDM system are used, the higher performance gain can be achieved. Simulations are provided to validate its advantages in both AWGN channel and time-varying multipath channel. We will investigate SSOP-OM technology for other multicarrier systems in the future.

ACKNOWLEDGMENT

The authors would like to thank the anonymous reviewers for their insightful comments and good suggestions that have significantly improved the quality of our manuscript.

REFERENCES

[1] A. R. S. Bahai and B. R. Saltzberg, *Multi-Carrier Digital Communications: Theory and Applications of OFDM* (Information Technology: Transmission, Processing and Storage). New York, NY, USA: Springer, 2004.
[2] S. Sesia, I. Toufik, and M. Baker, *LTE—The UMTS Long Term Evolution: From Theory to Practice*, 2nd ed. Chippenham, U.K.: Wiley, 2011.
[3] A. Ali and W. Hamouda, "Advances on spectrum sensing for cognitive radio networks: Theory and applications," *IEEE Commun. Surveys Tuts.*, vol. 19, no. 2, pp. 1277–1304, 2nd Quart., 2016.
[4] H. A. Mahmoud and H. Arslan, "Spectrum shaping of OFDM-based cognitive radio signals," in *Proc. IEEE Radio Wireless Symp*, Jan. 2008, pp. 113–116.
[5] H. Yamaguchi, "Active interference cancellation technique for MB-OFDM cognitive radio," in *Proc. 34th Eur. Microw. Conf.*, vol. 2, Oct. 2004, pp. 1105–1108.
[6] D. Qu, Z. Wang, and T. Jiang, "Extended active interference cancellation for sidelobe suppression in cognitive radio OFDM systems with cyclic prefix," *IEEE Trans. Veh. Technol.*, vol. 59, no. 4, pp. 1689–1695, May 2010.
[7] C.-D. Chung, "Spectrally precoded OFDM," *IEEE Trans. Commun.*, vol. 54, no. 12, pp. 2173–2185, Dec. 2006.
[8] J. F. Schmidt, S. Costas-Sanz, and R. López-Valcarce, "Choose your subcarriers wisely: Active interference cancellation for cognitive OFDM," *IEEE Trans. Emerg. Sel. Topics Circuits Syst.*, vol. 3, no. 4, pp. 615–625, Dec. 2013.
[9] P. Kryszkiewicz and H. Bogucka, "Out-of-band power reduction in NC-OFDM with optimized cancellation carriers selection," *IEEE Commun. Lett.*, vol. 17, no. 10, pp. 1901–1904, Oct. 2013.

[10] Z. Zhang, H. Wang, G. Yu, Y. Zhang, and X. Wang, "Universal filtered multi-carrier transmission with adaptive active interference cancellation," *IEEE Trans. Commun.*, vol. 65, no. 6, pp. 2554–2567, Jun. 2017.
[11] C. Ni, T. Jiang, and W. Peng, "Joint PAPR reduction and sidelobe suppression using signal cancelation in NC-OFDM-based cognitive radio systems," *IEEE Trans. Veh. Technol.*, vol. 64, no. 3, pp. 964–972, Mar. 2015.
[12] J. V. D. Beek and F. Berggren, "Out-of-band power suppression in OFDM," *IEEE Commun. Lett.*, vol. 12, no. 9, pp. 609–611, Sep. 2008.
[13] J. van de Beek and F. Berggren, "N-continuous OFDM," *IEEE Commun. Lett.*, vol. 13, no. 1, pp. 1–3, Jan. 2009.
[14] J. van de Beek, "Orthogonal multiplexing in a subspace of frequency well-localized signals," *IEEE Commun. Lett.*, vol. 14, no. 10, pp. 882–884, Oct. 2010.
[15] M. Ma, X. Huang, B. Jiao, and Y. J. Guo, "Optimal orthogonal precoding for power leakage suppression in DFT-based systems," *IEEE Trans. Commun.*, vol. 59, no. 3, pp. 844–853, Mar. 2011.
[16] X. Huang, J. A. Zhang, and Y. J. Guo, "Out-of-band emission reduction and a unified framework for precoded OFDM," *IEEE Commun. Mag.*, vol. 53, no. 6, pp. 151–159, Jun. 2015.
[17] C.-D. Chung and K.-W. Chen, "Spectrally precoded OFDM without guard insertion," *IEEE Trans. Veh. Technol.*, vol. 66, no. 1, pp. 107–121, Jan. 2017.
[18] H. Kawasaki, M. Ohta, and K. Yamashita, "Computational complexity reduction of orthogonal precoding for sidelobe suppression of OFDM signal," in *Proc. 21st Asia–Pacific Conf. Commun.*, Oct. 2015, pp. 460–463.
[19] I. V. L. Clarkson, "Orthogonal precoding for sidelobe suppression in DFT-based systems using block reflectors," in *Proc. IEEE Int. Conf. Acoust., Speech, Signal Process.*, Mar. 2017, pp. 3709–3713.
[20] H. Kawasaki, K. Ishizu, and F. Kojima, "Computationally efficient orthogonal precoding for sidelobe suppression of OFDM signals," in *Proc. IEEE Int. Conf. Commun.*, May 2018, pp. 1–6.
[21] H. Kawasaki, M. Ohta, and K. Yamashita, "Matrix decomposition of precoder matrix in orthogonal precoding for sidelobe suppression of OFDM signals," *IEICE Trans. Commun.*, vol. E101.B, no. 7, pp. 1716–1722, Jul. 2018.
[22] J. A. Zhang, X. Huang, A. Cantoni, and Y. J. Guo, "Sidelobe suppression with orthogonal projection for multicarrier systems," *IEEE Trans. Commun.*, vol. 60, no. 2, pp. 589–599, Feb. 2012.
[23] X. Huang, Y. J. Guo, A. Zhang, and V. Dyadyuk, "A multi-gigabit microwave backhaul," *IEEE Commun. Mag.*, vol. 50, no. 3, pp. 122–129, Mar. 2012.
[24] A. Goldsmith, *Wireless Communications*. Cambridge, U.K.: Cambridge Univ. Press, Aug. 2005.
[25] B. Korte and J. Vygen, *Combinatorial Optimization*. Amsterdam, The Netherlands: Elsevier, 2005.
[26] P. Hoeher, "A statistical discrete-time model for the WSSUS multipath channel," *IEEE Trans. Veh. Technol.*, vol. 41, no. 4, pp. 461–468, Nov. 1992.

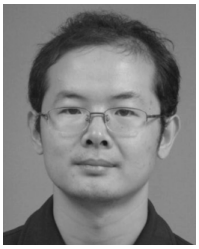

GUANGFA DAI received the B.S. degrees in physics and electrical engineering from Hubei University, Wuhan, China, in 2001, and the M.S. degree in biomedical engineering from South Central University for Nationalities, Wuhan, in 2005. He is currently pursuing the Ph.D. degree with the School of Electronic Information, Wuhan University, Wuhan. He is also with the Hubei Key Laboratory of Intelligent Wireless Communications, South Central University for Nationalities. His main research interests include communication signal processing, wireless communication systems, and cognitive radio.

SHAOPING CHEN received the B.S. and M.S. degrees in electrical engineering from Wuhan University, Wuhan, China, in 1987 and 1990, respectively, and the Ph.D. degree in information and communication engineering from the Huazhong University of Science and Technology, Wuhan, in 2004. He is currently a Professor with the Hubei Key Laboratory of Intelligent Wireless Communications, South Central University for Nationalities, Wuhan. His research interests include the communications and signal processing, including transceiver design, detection and estimation, and wireless and optical communication systems.

GAOFENG WANG (S'93–M'95–SM'01) received the Ph.D. degree in electrical engineering from the University of Wisconsin, Milwaukee, in 1993, and the Ph.D. degree in scientific computing from Stanford University, Stanford, CA, USA, in 2001.

From 1993 to 1996, he was a Scientist at Tanner Research Inc., Pasadena, CA, USA. From 1996 to 2001, he was a Principal Research and Development Engineer with Synopsys Inc., Mountain View, CA, USA. In 1999, he was a Consultant at Bell Laboratories, Murray Hill, NJ, USA. From 2001 to 2003, he was the Chief Technology Officer (CTO) with Intpax, Inc., San Jose, CA, USA. From 2004 to 2010, he was the CTO with Siargo Inc., Santa Clara, CA, USA. From 2010 to 2013, he was a Chief Scientist at Lorentz Solution, Inc., Santa Clara, CA, USA. From 2004 to 2013, he was an Adjunct Professor and the Founding Director of the Institute of Microelectronics and Information Technology, Wuhan University, Hubei, China. He is currently a Distinguished Professor with the School of Electronics and Information, Hangzhou Dianzi University, Zhejiang, China. He has published over 400 peer-reviewed journal articles and conference papers. He holds over 40 patents. His research and development interests include integrated circuits, MEMS and sensor technology, electronic design automation, and computational electromagnetics.

Dr. Wang is a Fellow of the Institution of Engineering and Technology.